Interaction of brassinosteroid and cytokinin promotes ovule initiation and increases seed number per silique in *Arabidopsis*[oo]

Song-Hao Zu[1,2†] [iD], Yu-Tong Jiang[1†] [iD], Jin-Hui Chang[1] [iD], Yan-Jie Zhang[1] [iD], Hong-Wei Xue[2] [iD] and Wen-Hui Lin[1,2*] [iD]

1. School of Life Sciences and Biotechnology, The Joint International Research Laboratory of Metabolic and Developmental Sciences, Joint Center for Single Cell Biology, Shanghai Jiao Tong University, Shanghai 200240, China
2. School of Agriculture and Biology, Joint Center for Single Cell Biology, Shanghai Jiao Tong University, Shanghai 200240, China
[†]These authors contributed equally to this work.
*Correspondence: Wen-Hui Lin (whlin@sjtu.edu.cn)

Song-Hao Zu

Wen-Hui Lin

ABSTRACT

Ovule initiation is a key step that strongly influences ovule number and seed yield. Notably, mutants with enhanced brassinosteroid (BR) and cytokinin (CK) signaling produce more ovules and have a higher seed number per silique (SNS) than wild-type plants. Here, we crossed BR- and CK-related mutants to test whether these phytohormones function together in ovule initiation. We determined that simultaneously enhancing BR and CK contents led to higher ovule and seed numbers than enhancing BR or CK separately, and BR and CK enhanced each other. Further, the BR-response transcription factor BZR1 directly interacted with the CK-response transcription factor ARABIDOPSIS RESPONSE REGULATOR1 (ARR1). Treatments with BR or BR plus CK strengthened this interaction and subsequent ARR1 targeting and induction of downstream genes to promote ovule initiation. Enhanced CK signaling partially rescued the reduced SNS phenotype of BR-deficient/insensitive mutants whereas enhanced BR signaling failed to rescue the low SNS of CK-deficient mutants, suggesting that BR regulates ovule initiation and SNS through CK-mediated and -independent pathways. Our study thus reveals that interaction between BR and CK promotes ovule initiation and increases seed number, providing important clues for increasing the seed yield of dicot crops.

Keywords: brassinosteroid, cytokinin, ovule initiation, protein interaction, seed number per silique

INTRODUCTION

Seed number and weight determine seed yield. Studies on the regulation of seed yield have focused mainly on seed development and seed weight (Schou et al., 1978; Liu et al., 2006; Song et al., 2007), with less attention given to seed number because an increase in seed number was presumed to lead to decreased seed weight due to nutrient and space limitations (Kiniry et al., 1990). However, recent reports indicate that seed weight and number can be simultaneously increased to improve yield (Bartrina et al., 2011; Huang et al., 2013; Jiang et al., 2013; Monpara and Gaikwad, 2014).

The regulation of seed number has been investigated in some cereal crops (Schou et al., 1978; Kiniry et al., 1990; Jiang

and Egli, 1995; Liu et al., 2006; Gambín and Borrás, 2010), but little is known about this process in dicots. In the model dicot plant *Arabidopsis thaliana*, total seed number depends on the number of siliques and the seed number per silique (SNS). The SNS is affected by developmental processes including ovule initiation and development, male and female gametophyte development, fertilization, and zygote development (Chaudhury et al., 1997). Plant hormones are involved in nearly all aspects of plant growth and reproduction. The number of ovules ultimately determines the maximum SNS. Notably, two phytohormone-related mutants, *ckx3 ckx5* (Bartrina et al., 2011) and *bzr1-1D* (He et al., 2002; Huang et al., 2013; Jiang et al., 2013), with enhanced brassinosteroid (BR) and cytokinin (CK) signaling, respectively, show significantly increased SNS, indicating that these phytohormones function in ovule initiation and SNS regulation.

The signal transduction pathways for both CK and BR have been well studied in *Arabidopsis* (Purohit, 1985; Bartrina et al., 2011; Huang et al., 2013; Cucinotta et al., 2014). CK promotes cell division and differentiation (Morris et al., 1999; Rin et al., 2002; Takatoshi et al., 2003; Higuchi et al., 2004; Jennifer et al., 2004; Ferreira and Kieber, 2005). CK degradation is catalyzed by CK oxidase/dehydrogenase (CKX), which maintains CK homeostasis *in vivo* (Morris et al., 1999; Rin et al., 2002). CK signals are transported via ARABIDOPSIS HISTIDINE PROTEINs to ARABIDOPSIS RESPONSE REGULATORs (ARRs) (Takatoshi et al., 2003; Jennifer et al., 2004; Ferreira and Kieber, 2005; Sakakibara, 2006; Liu et al., 2017), with B-ARRs acting as positive transcriptional regulators in the CK signaling pathway (Takatoshi et al., 2003; Mason et al., 2005). BR is involved in cell elongation and division, cell and tissue differentiation and organogenesis, and photomorphogenesis and responses to the environment (Grove et al., 1979; Clouse et al., 1996; Clouse and Sasse, 1998; Fujioka and Yokota, 2003). Upon binding BR, an active receptor complex transports the BR signal to inhibit BRASSINOSTEROID INSENSITIVE2 (BIN2) (Li et al., 2001; He et al., 2002) and releases the BR-induced transcription factors BRASSINAZOLE-RESISTANT 1 (BZR1) and BRASSINAZOLE RESISTANT 2 (BES1) (Wang et al., 2002; He et al., 2005; Huang et al., 2013), which regulate the expression of downstream genes (Wang et al., 2002; He et al., 2005). When the BR level increases, BZR1 is activated and inhibits the expression of biosynthetic genes, which leads to feedback inhibition of BR signaling (He et al., 2002, 2005; Wang et al., 2002, 2012).

Phytohormones including CK and BR influence floral organ development, which is regulated by the ABCDE genes which refers to four-whorl development of floral organs and ovules. Among them, class D genes control ovule identity and ovule primordia initiation, and encode transcription factors and regulatory proteins such as *SEEDSTICK* (STK) and *SHATTERPROOF 1/2* (SHP1/2) (Weige and Meyerowitz, 1994; Favaro et al., 2003). The triple mutant of *ARABIDOPSIS HISTIDINE KINASE* (AHK), *ahk1-12 ahk2-2 ahk3-3*, produces fewer ovules than the wild type. Conversely, the CK-enhanced mutant *ckx3 ckx5* produces more lateral branches,

larger floral organs, and denser inflorescence apices and ovules, with increased SNS (Ferreira and Kieber, 2005; Mizuno, 2005; Liu et al., 2017), compared to the wild type. We previously reported that BR-deficient and BR-insensitive mutants show reduced ovule numbers and SNS (Huang et al., 2013), while the gain-of-function mutant of BZR1 (*bzr1-1D*) shows increased ovule number and SNS, suggesting that BR positively regulates ovule initiation and development, as well as SNS. Additional study demonstrated that BR positively regulates genes that promote early ovule development, such as *AINTEGUMENTA* (ANT) and *HUELLENLOS* (HLL) (Schneitz et al., 1998), and negatively regulates genes that inhibit early ovule development, such as *APETALA2* (AP2), ultimately enhancing SNS (Galbiati et al., 2013).

In this study, we analyzed BR- and CK-related mutants to investigate their regulation of ovule initiation and SNS. We observed cross-talk between BR and CK, such that enhancing both signals simultaneously promoted ovule initiation and increased the SNS more efficiently than enhancing them separately. We further demonstrated a direct protein-level interaction between the key transcription factors related to these two hormones, BZR1 and ARR1. This interaction affected the transcription of downstream genes involved in ovule initiation. Our study thus establishes that BR and CK work together to regulate ovule initiation and SNS, and identifies candidate genes for increasing seed number and yield which has both scientific significance and potential applications for increasing crop yield.

RESULTS

BR and CK positively regulate *Arabidopsis* growth and increase ovule and seed number

We previously demonstrated that BR positively regulates ovule and seed numbers (Huang et al., 2013; Yu et al., 2020), and that CK is also involved in these processes (Bartrina et al., 2011; Huang et al., 2013; Jiang et al., 2013). In this study, we investigated the effect of cross-talk between BR and CK on ovule initiation and SNS. First, we examined the effect of CK alone and observed that loss-of-function mutants of ARRs (single, double, and triple mutants of ARR1, ARR10, and ARR12; *arr1 10 12*) with decreased CK signaling had reduced SNS (Figure S1A), while the *ckx3 ckx5* double mutant, with enhanced CK content, produced enlarged rosette leaves (before bolting) (Figure 1A, B) and flowers, increased main inflorescence stem height (Figure 1C), enlarged siliques (Figure 1D), and increased SNS (Figure 1E), which was consistent with previous studies. We assessed the expression of CK response regulator marker genes (*ARR5* and *ARR7*) in inflorescence apices of *ckx3 ckx5* plants using quantitative reverse transcription polymerase chain reaction (qRT-PCR) and observed upregulated expression, as expected (Figure S1B). qRT-PCR data also showed induction of *STK* and *SHP1/2*, positive regulators of ovule initiation (Bartrina et al., 2011), indicating that CK regulates ovule initiation through inducing the expression of positive regulators of ovule identity and initiation.
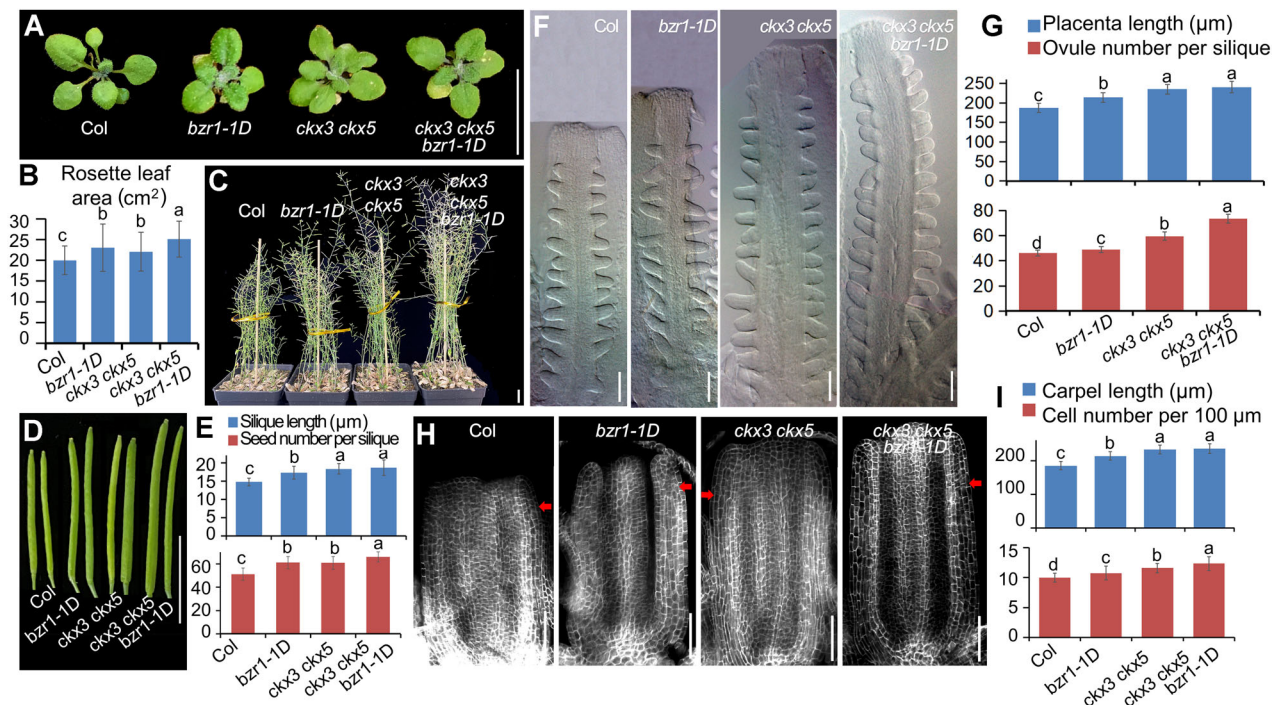
Figure 1. Brassinosteroid (BR) and cytokinin (CK) positively regulate *Arabidopsis* growth and increase the seed number per silique (SNS)

(**A**) Seedlings (21 d after germination: DAG) and (**B**) statistics of leaf area of rosette leaves before bolting of wild type (Col), *bzr1-1D*, *ckx3 ckx5*, and *ckx3 ckx5 bzr1-1D* (scale bars, 1 cm). (**C**) Adult plants of wild type (Col), *bzr1-1D*, *ckx3 ckx5*, and *ckx3 ckx5 bzr1-1D* (scale bars, 1 cm). (**D**) and (**E**) Siliques of Col, *bzr1-1D*, *ckx3 ckx5*, and *ckx3 ckx5 bzr1-1D* (scale bars, 1 cm) and statistical analysis of silique length and SNS. Bars represent mean $\pm$ SD of three biological replicates ($n = 30$). Lowercase letters indicate statistically significant differences between different stages ($P < 0.05$). (**F**) Placenta and ovules in flowers at developmental stage 9 of Col, *bzr1-1D*, *ckx3 ckx5*, and *ckx3 ckx5 bzr1-1D* (scale bars, 50 μm) and (**G**) statistical analysis of placenta length and ovule number. Bars represent mean $\pm$ SD of three biological replicates ($n = 15$). Lowercase letters indicate statistically significant differences between different stages ($P < 0.05$). (**H**) Pistils in flowers at developmental stage 8 of Col, *bzr1-1D*, *ckx3 ckx5*, and *ckx3 ckx5 bzr1-1D* (scale bars, 50 μm) and (**I**) statistical analysis of pistil length (cell layers were counted at position of red arrows) and cell numbers. Bars represent mean $\pm$ SD of three biological replicates ($n = 30$). Lowercase letters indicate statistically significant differences between different stages ($P < 0.05$).

We next examined BR signaling; the *bzr1-1D* mutant, with enhanced BR levels, exhibited enlarged rosette leaves (Figure 1A, B), a taller main inflorescence stem (Figure 1C), larger flowers, larger siliques (Figure 1D), and increased SNS (Figure 1E), which was consistent with published data (Wang et al., 2002). To explore how BR affects ovule and seed numbers, we examined the expression of *CONSTITUTIVE PHO-TOMORPHOGENIC DWARF* (*CPD*) and *DWARF 4* (*DWF4*), two BR biosynthesis genes negatively regulated by BR (Fujioka and Yokota, 2003; Ohnishi et al., 2012), using qRT-PCR, and both were downregulated in the *bzr1-1D* mutant as expected (Figure S1C). The expression of *AP2*, the negative regulator of ovule identity and initiation, was repressed, while that of *SHP1/2*, positive regulators of ovule identity and initiation, was upregulated in the mutant, suggesting that BR regulates ovule initiation through repressing the negative regulator and inducing the positive regulator of ovule identity and initiation (Figure S1C), consistent with our previous data. Moreover, the expression of three positive regulators of ovule identity and initiation, *STK*, *ANT*, and *HLL*, was induced by treatment with 1 μmol/L epi-brassinolide (eBL) or 1 μmol/L 6-benzylamin-opurine (6-BA), indicating again that BR and CK influence

ovule number through transcriptional regulation of genes involved in ovule initiation (Figure S1D).

To investigate the cross-talk between BR and CK in plant development and SNS, we crossed the *bzr1-1D* mutant with the *ckx3 ckx5* mutant and obtained the triple mutant *ckx3 ckx5 bzr1-1D*. The adult triple mutant plants exhibited similar main inflorescence stem heights (Figure 1C) and similar silique lengths (Figure 1D, E) as *ckx3 ckx5* plants, but significantly larger rosette leaves (Figure 1A, B) and increased SNS (Figure 1E). These phenotypes indicated that simultaneously enhancing BR and CK signals increased the SNS more efficiently than enhancing them separately. *bzr1-1D* and *ckx3 ckx5* displayed longer pistils and more ovules (Figure 1F, G) than the wild type, and the *ckx3 ckx5 bzr1-1D* triple mutant had more ovules than *bzr1-1D* and *ckx3 ckx5* (Figure 1G). In addition, the ovules in the *ckx3 ckx5 bzr1-1D* placentae were crowded with almost no gaps between them. Furthermore, *bzr1-1D* and *ckx3 ckx5* had a longer placenta (Figure 1F, G) than the wild type, indicating that BR and CK positively regulate placenta elongation. To explore the role of BR and CK in ovule primordia protrusion, we counted cell numbers in the outermost layer of the pistil at floral stage 8 and observed 27% more cells in *ckx3*

ckx5 bzr1-1D (Figure 1H–I) than in the wild type, 10% more cells than in *ckx3 ckx5*, and 11% more cells than in *bzr1-1D*, indicating that BR and CK coordinately promote cell division and pistil and placenta elongation.

Since BR and CK positively regulate ovule and seed development (He et al., 2002; Wang et al., 2002, 2012; Bartrina et al., 2011; Huang et al., 2013; Jiang et al., 2013) and do not affect fertility, the enhanced placenta length and ovule primordium initiation led to increased numbers of ovules and SNS in the above mutants. Therefore, we conclude that BR and CK positively regulate ovule and seed number by promoting placenta elongation and ovule primordia initiation.

BR and CK signals enhance each other

The qRT-PCR analyses using wild-type *Arabidopsis* inflorescence apices demonstrated that *ARR5* and *ARR7*, two positive CK marker genes, were upregulated by 10 nmol/L eBL treatment, indicating that enhancing BR signaling promotes the CK response (Figure 2A). The fluorescence signal in the CK marker line, TCS:GFP, was increased in the placenta and ovule in the *bzr1-1D* background but decreased in the *bin2⁺/⁻* background, indicating that BR positively regulates the CK response (Figures 2B, C, S2). Western blot analyses also showed a significant increase and decrease of TCS:GFP in *bzr1-1D* and *bin2⁺/⁻* backgrounds (Figure 2D), respectively, further confirming that enhanced BR signaling upregulates the CK response.

Similarly, downregulation of the BR negative marker genes (*CPD* and *DWF4*) by 6-BA treatment suggested that CK also induces the BR response (Figure 3A). The fluorescence signal of nucleus-localized BZR1 was increased in the *ckx3 ckx5* background, indicating that BZR1 activity was increased by 6-BA treatment in the mutant as compared with the wild type (Figure 3B, C). The BZR1 protein level was increased in the *ckx3 ckx5* background as compared with the wild type, suggesting that the 6-BA treatment induces BZR1 accumulation and the increased CK level possibly promotes the BR response (Figure 3B, C). Together, our results implied that BR and CK signals enhance each other.

BR promotes direct interaction of BZR1 and ARR1

BZR1 interacts with components of other signaling pathways to integrate BR and other signals (He et al., 2005; Wang et al., 2002, 2012). To investigate whether BZR1 mediates the integration of BR and CK, we conducted yeast two-hybrid assays and determined that BZR1 interacted with the CK-response transcription factors ARR1 and ARR10 (Figures 4A, S3A). Bimolecular fluorescence complementation (BiFC) assays revealed that BZR1 interacts with ARR1 in the nucleus (Figure 4D) but does not interact with ARR10 (Figure S3B). Using the tobacco transient expression system, we observed that BZR1 and ARR1 co-localize in the nucleus, and this co-localization was
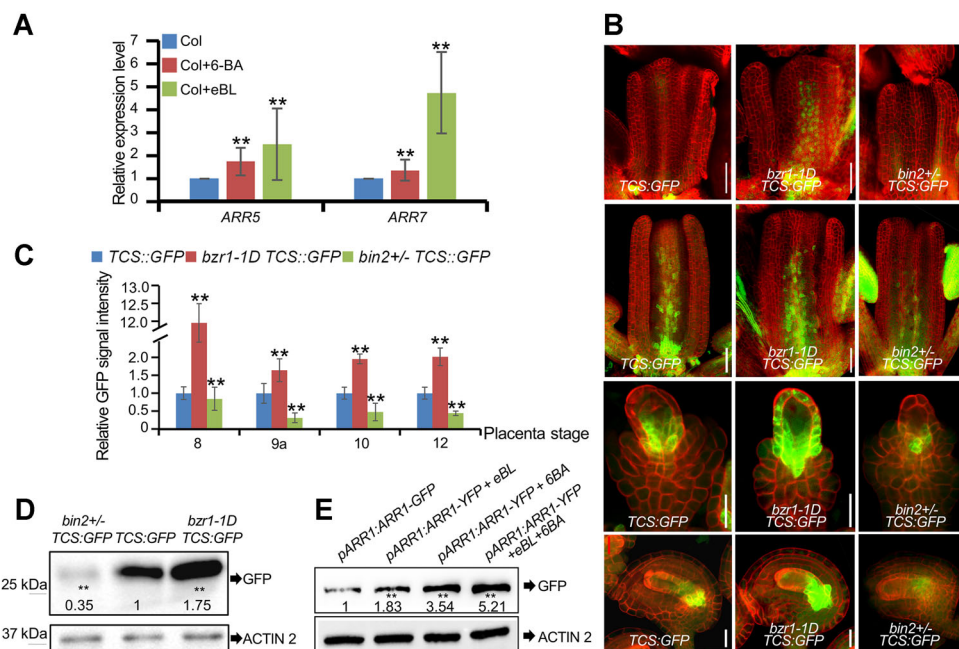
Figure 2. Brassinosteroid (BR) enhances cytokinin (CK) signaling
(**A**) Relative transcript levels of *ARR5* and *ARR7* under 1 μmol/L eBL and 1 μmol/L 6-BA treatment. (**B**) Fluorescence signal of *TCS:GFP* (CK signaling reporter) in placenta (scale bars, 50 μm) and ovules (scale bars, 20 μm) of Col, *bzr1-1D*, and *bin2⁺/⁻*. Graphs represent typical phenotype of all samples. (**C**) Quantitative analysis of *TCS:GFP* fluorescence level in placenta and ovules. Bars correspond to relative GFP signal intensity. Relative fluorescence signal data were extracted from normalized mean gray levels in above lines. Values correspond to arithmetic means ± SE of three biological replicates ($n = 20$). Asterisks indicate significant difference (Student's two-tailed *t*-test: **$P < 0.01$). (**D**) GFP protein level in inflorescence apices of above plants. (**E**) ARR1-GFP protein level in *pARR1:ARR1-GFP* stably transformed line under 1 μmol/L eBL, 1 μmol/L 6-BA treatment and co-treatment of 1 μmol/L eBL+ 1 μmol/L 6-BA. Graphs represent typical phenotype of all samples. A quantitative analysis of GFP protein levels is shown below the band in the blot. Bands in blots correspond to arithmetic means ± SD of three biological replicates ($n = 3$). Asterisks indicate significant difference (Student's two-tailed *t*-test: **$P < 0.01$).
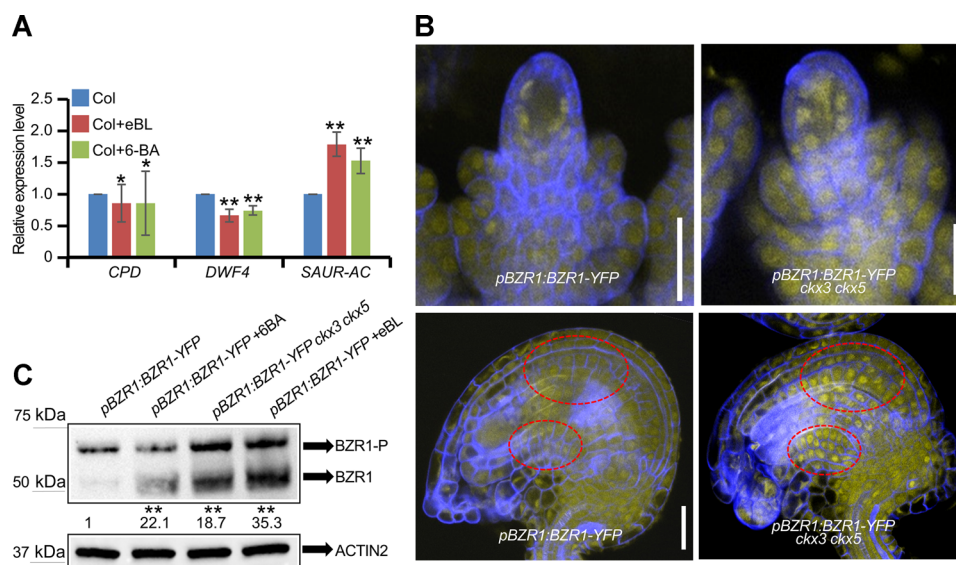
Figure 3. Cytokinin (CK) enhances brassinosteroid (BR) signaling

(**A**) Relative transcript levels of *CPD*, *DWF4*, and *SAUR-AC* under 1 μmol/L eBL and 1 μmol/L 6-BA treatment. (**B**) Fluorescence signal of *pBZR1:BZR1-YFP* (BR signaling reporter) in ovules of Col, *bzr1-1D*, and *bin2+/−* (scale bars, 20 μm). eBL treatment concentration is 1 μmol/L. Graphs represent typical phenotype of all samples. The red circle refers to the fluorescence located in the nucleus. Quantitative analysis of BZR1-YFP fluorescence level is shown in picture (*n* = 15). (**C**) Phosphorylation (BZR1-P) and dephosphorylation (BZR1) of BZR1-YFP protein level in inflorescence apices of *pBZR1:BZR1-YFP* and *pBZR1:BZR1-YFP ckx3 ckx5* stably transformed line. eBL and 6-BA treatment concentration is 1 μmol/L. Numbers below the figure show the ratio of dephosphorylation BZR1 to phosphorylation BZR1. Graphs represent typical phenotype of all samples. A quantitative analysis of YFP protein levels is shown below the band in the blot. Bands in blots correspond to arithmetic means ± SD of three biological replicates (*n* = 3). Asterisks indicate significant difference (Student's two-tailed *t*-test: **$P < 0.01$).

enhanced by 100 nmol/L eBL (Figure 4B, C). We also established that BZR1 interacts with ARR1 in a co-immunoprecipitation (Co-IP) assay (Figures 4E, S3A) and *in vitro* pull-down assays in *Escherichia coli* (Figure 4F). Co-IP assays revealed that BR treatment alone and co-treatment with CK increased the BZR1 and ARR1 protein levels as well as the BZR1–ARR1 interaction (Figure S3C). Using *Arabidopsis* inflorescence apices containing pARR1:ARR1-GFP in the Co-IP assay to enhance the accuracy of the experiment, we observed that BR treatment alone and co-treatment with CK increased the BZR1–ARR1 interaction (Figure S3D). Considering that BR treatment enhanced the ratio of dephosphorylated BZR1 (localized in the nucleus) (Wang et al., 2002) (Figure S3C), and that BZR1 and ARR1 co-localized in the nucleus (Figure 4B, C), we hypothesize that ARR1 interacts with dephosphorylated BZR1 in the nucleus.

These *in vitro* and *in vivo* experiments demonstrated that the interplay between BZR1 and ARR1 in the nucleus increases BR levels, which, in turn, enhances the BZR1–ARR1 interaction.

Transcriptome analysis identified downstream genes involved in ovule identity and initiation

Our experiments indicated that the increase in SNS in the *bzr1-1D*, *ckx3 ckx5*, and *ckx3 ckx5 bzr1-1D* mutants resulted from elongated placentae and increased ovule initiation. To identify genes involved in regulating placenta development and initiation of ovule primordia, we performed RNA-Seq

using gynoecia of flowers at developmental stage 8 collected from wild-type (Col), *bzr1-1D*, *ckx3 ckx5*, and *ckx3 ckx5 bzr1-1D* plants. To avoid interference, we removed the stigma and junction parts of flower organs before extracting total RNA and identified differentially expressed genes (DEGs), including some associated with several metabolic and hormone signal transduction pathways (Figure 5A). Among them, 513 DEGs were specifically regulated by BR, 337 by CK, and 1,270 by BR and CK together (Figure 5B–E). There were 18 commonly upregulated genes and 189 commonly downregulated genes in *bzr1-1D* and *ckx3 ckx5*, respectively (Figure 5C). However, only one gene was upregulated in *ckx3 ckx5* but downregulated in *bzr1-1D*, and no genes were upregulated in *bzr1-1D* but downregulated in *ckx3 ckx5* (Figure 5C–E).

The significant downregulation of *CPD* and *DWF4* in *bzr1-1D* indicated enhanced BR signaling in this mutant (Dataset S1), while the significant upregulation of *ARR15* in the *ckx3 ckx5* mutant indicated enhanced CK signaling. Notably, significant downregulation of *DWF4* and significant upregulation of *ARR5* in the *ckx3 ckx5 bzr1-1D* triple mutant indicated enhanced BZR1 activity and increased CK levels (Dataset S1). In addition, *STK* was upregulated in the *ckx3 ckx5* mutant, and much more upregulated in *ckx3 ckx5 bzr1-1D* plants, which suggested that increased CK levels positively regulate ovule primordia initiation through promoting *STK* expression, and that the enhanced BR signaling amplifies the effect of CK (Figure 5F; Dataset S1). Furthermore,

the downregulation of *AP2* in the *bzr1-1D* mutant indicated that enhanced BZR1 activity promotes ovule primordia initiation through repressing the expression of this negative regulator (Figure 5F; Dataset S1) (Galbiati et al., 2013). The transcript levels of *HLL* and *SHP2* were not significantly changed in *bzr1-1D* and *ckx3 ckx5* plants but were significantly upregulated in the *ckx3 ckx5 bzr1-1D* mutant, suggesting that BR and CK coordinately promote ovule initiation by inducing the expression of these positive regulators (Figure 5F; Dataset S1). These changes in the transcript levels of ovule identity and initiation genes in the *bzr1-1D* and *ckx3 ckx5* backgrounds suggested that our transcriptome analysis was reliable. We identified new genes involved in ovule initiation that respond to BR and CK signals to regulate SNS. Our transcriptomic data indicated that BR and CK coregulate placenta development and ovule primordia initiation by coregulating downstream genes.

BR and CK interaction increases the transcription of positive regulators of ovule initiation

ARR1 and BZR1 are key transcription factors in CK and BR pathways and have a positive regulatory effect on downstream genes (including ovule initiation regulatory genes), such as ARR1 target genes *WUSCHEL* (*WUS*), *STK*, and *HLL*, and the BZR1 target gene *DWF4*. CK and BR regulate plant growth and development (including ovule initiation) through activating ARR1 and BZR1, respectively, to target and regulate the transcription of downstream genes. To study whether the coordination of BR and CK is more effective than their individual effects on the regulation of positive regulators of ovule initiation, we used *WUS*, *STK*, *HLL*, and *DWF4* as marker genes in a dual LUC assay.

WUS is involved in regulation of plant development (including ovule development) (Groß-Hardt et al., 2002). We conducted chromatin immunoprecipitation (ChIP) and LUC assays using *WUS* as a positive control because *WUS* is targeted and induced by ARR1 but not by BZR1 (Sun et al., 2010). The ChIP result confirmed this, and showed that the targeting of *WUS* by ARR1 is enhanced by CK treatment alone and by co-treatment with BR (Figure 6A, B). Although ChIP assay was carried out in seedlings, the same conclusion could be obtained in ovule samples. Conversely, *DWF4* is targeted by BZR1 but not ARR1 (Xie et al., 2018). Our ChIP assay showed that BR treatment enhanced the
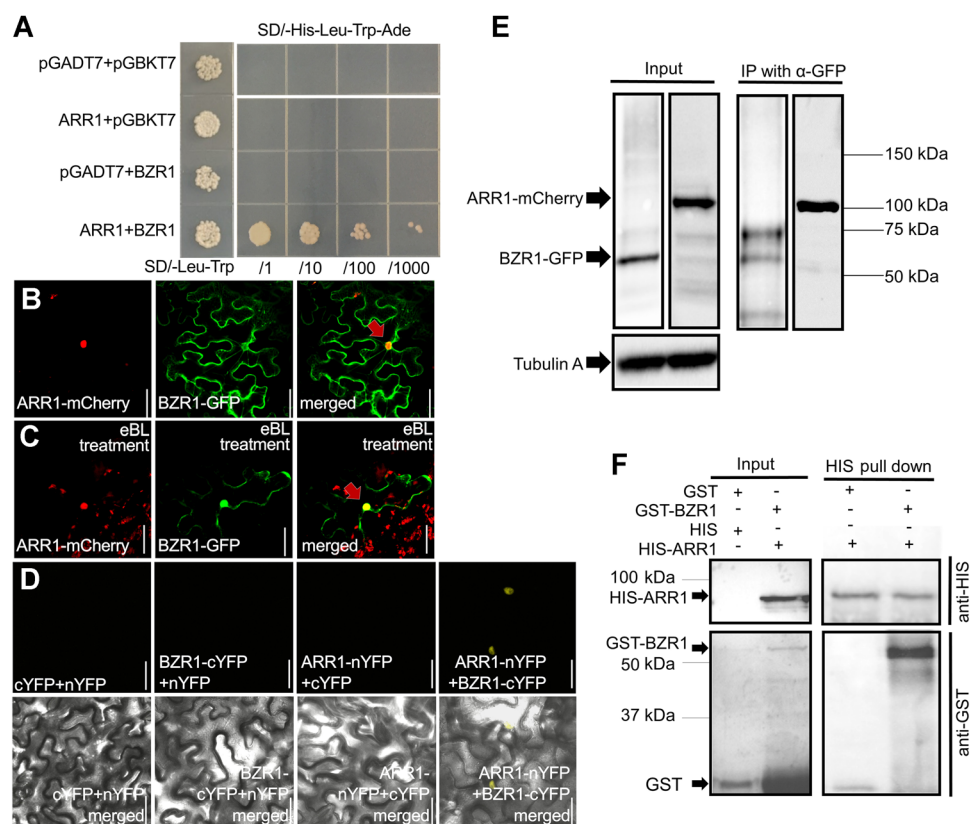
Figure 4. BRASSINAZOLE-RESISTANT 1 (BZR1) directly interacts with REGULATOR1 (ARR1)

(**A**) Yeast two-hybrid assay showing that ARR1 interacts with BZR1. (**B**) Confocal images of tobacco epidermal cells co-expressing ARR1-mcherry and BZR1-GFP (scale bar, 100 μm). The red arrow refers to the co-localization of the two proteins. (**C**) Confocal images of tobacco epidermal cells co-expressing ARR1-mcherry and BZR1-GFP under 100 nmol/L eBL treatment (scale bar, 100 μm). The red arrow refers to the enhanced co-localization of the two proteins. (**D**) Bimolecular fluorescence complementation analyses of interaction between ARR1 and BZR1 (scale bar, 50 μm). (**E**) Co-Immunoprecipitation (Co-IP) assays confirmed that BZR1-GFP interact with ARR1-mCherry in tobacco leaves. (**F**) *In vitro* pull-down assays demonstrating direct interaction between HIS-ARR1 and GST-BZR1.

targeting of *DWF4* by BZR1, and co-treatment with CK strengthened this interaction, indicating that CK enhances the BR-induced targeting of *DWF4* by BZR1. In addition, the expression of *PUTATIVE INCREASED SNS1* (*INS1*; *At1G68440*), which has not been characterized, was induced in *bzr1-1D*, *ckx3 ckx5*, and *ckx3 ckx5 bzr1-1D* in our transcriptome analysis. Our ChIP analysis showed that BZR1 targets *INS1*, and this targeting was enhanced by BR treatment but not by co-treatment with CK, indicating BR-specific regulation of *INS1*.

To further determine whether BZR1 aids in ARR1 activation of *WUS*, we performed transient expression assays in the tobacco transient expression system with *pWUS*:LUC, *pSTK*:LUC, and *pHLL*:LUC as reporters using a dual LUC system. Overexpression of *ARR1* and *BZR1-1D* (containing the same point mutation as in the *bzr1-1D* mutant, causing increased BR signaling) (He et al., 2002) resulted in a two-fold increase in *pWUS*:LUC activity (Figure 6D). Overexpression of *ARR1* alone resulted in an increase of *pSTK*:LUC and *pHLL*:LUC activity (Figure 6D). And overexpression of *ARR1* and *bzr1-1D* resulted in a two-fold increase in *pSTK*:LUC and *pHLL*:LUC activity (Figure 6D). These results suggest that BZR1

strengthens the ARR1-mediated induction of downstream genes to regulate ovule initiation and SNS.

## BR regulates the SNS partially through a CK-mediated pathway

Based on the phenotypes of the *bzr1-1D ckx3 ckx5* mutant with enhanced BR and CK signals, we hypothesized that BR and CK cooperate to promote ovule initiation and increase the SNS. To investigate their cross-talk under reduced BR and CK signaling, we crossed the *ckx3 ckx5* mutant with the BR-deficient or -insensitive mutants *det2*, *bin2*^{+/−}, and *bin2*^{−/−} (Figures 7A, S4A). Enhanced CK partially rescued the SNS in BR-deficient or -insensitive mutants (Figures 7, S4B). The SNS for *det2*, *bin2*^{+/−}, and *bin2*^{−/−} were 33, 34, and 3, respectively, while the SNS for the *det2 ckx3 ckx5*, *bin2*^{+/−}*ckx3 ckx5*, and *bin2*^{−/−}*ckx3 ckx5* mutants were significantly higher at 39, 49, and 6, respectively (Figures 7C, S4B).

We constructed *35S:CKX3* transgenic lines overexpressing the CK metabolic enzyme CKX3 (Rin et al., 2002). Transgenic plants showed severe CK deficiency phenotypes, including poor growth and dramatically decreased SNS (Figure 7B, C). We crossed two BR-signal-enhanced plant lines, *DWF4-OX*
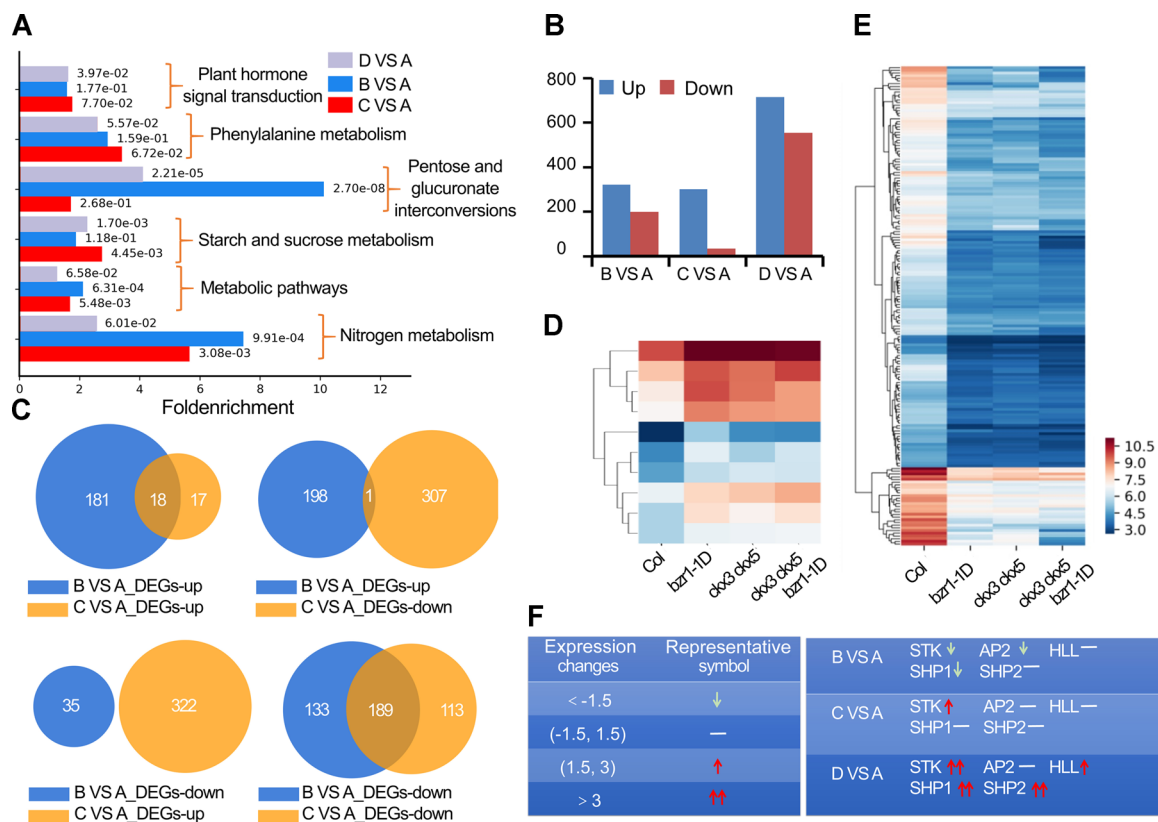
Figure 5. Transcriptomic analyses of placenta of *bzr1-1D*, *ckx3 ckx5*, and *ckx3 ckx5 bzr1-1D*
(**A**) Gene ontology (GO) analysis for genes. Differentially expressed gene (DEG) analysis (**B**) and venn diagram (**C**) showing number of overlapping up- and downregulated in *bzr1-1D* (represented by letter B) and *ckx3 ckx5* (represented by letter C) compared with wild type (Col-0) (represented by letter A) under control conditions. (**D**) Expression levels of DEGs (upregulated in *bzr1-1D* vs. Col, *ckx3 ckx5* vs. Col, and *ckx3 ckx5 bzr1-1D* vs. Col) in Col, *bzr1-1D*, *ckx3 ckx5*, and *ckx3 ckx5 bzr1-1D*. (**E**) Expression level of DEGs (downregulated in *bzr1-1D* vs. Col, *ckx3 ckx5* VS. Col, and *ckx3 ckx5 bzr1-1D* vs. Col) in Col, *bzr1-1D*, *ckx3 ckx5*, and *ckx3 ckx5 bzr1-1D*. (**F**) Tables show expression changes of ovule initiation regulating genes in *bzr1-1D* VS Col, *ckx3 ckx5* VS Col, and *ckx3 ckx5 bzr1-1D* VS Col. The calculation methods for expressing changes are as follow: $2^{(lgB-lgA)}$, $2^{(lgC-lgA)}$, $2^{(lgD-lgA)}$ in *bzr1-1D* (represented by letter B) versus Col, *ckx3 ckx5* (represented by letter C) versus Col, and *ckx3 ckx5 bzr1-1D* (represented by letter D) versus Col.
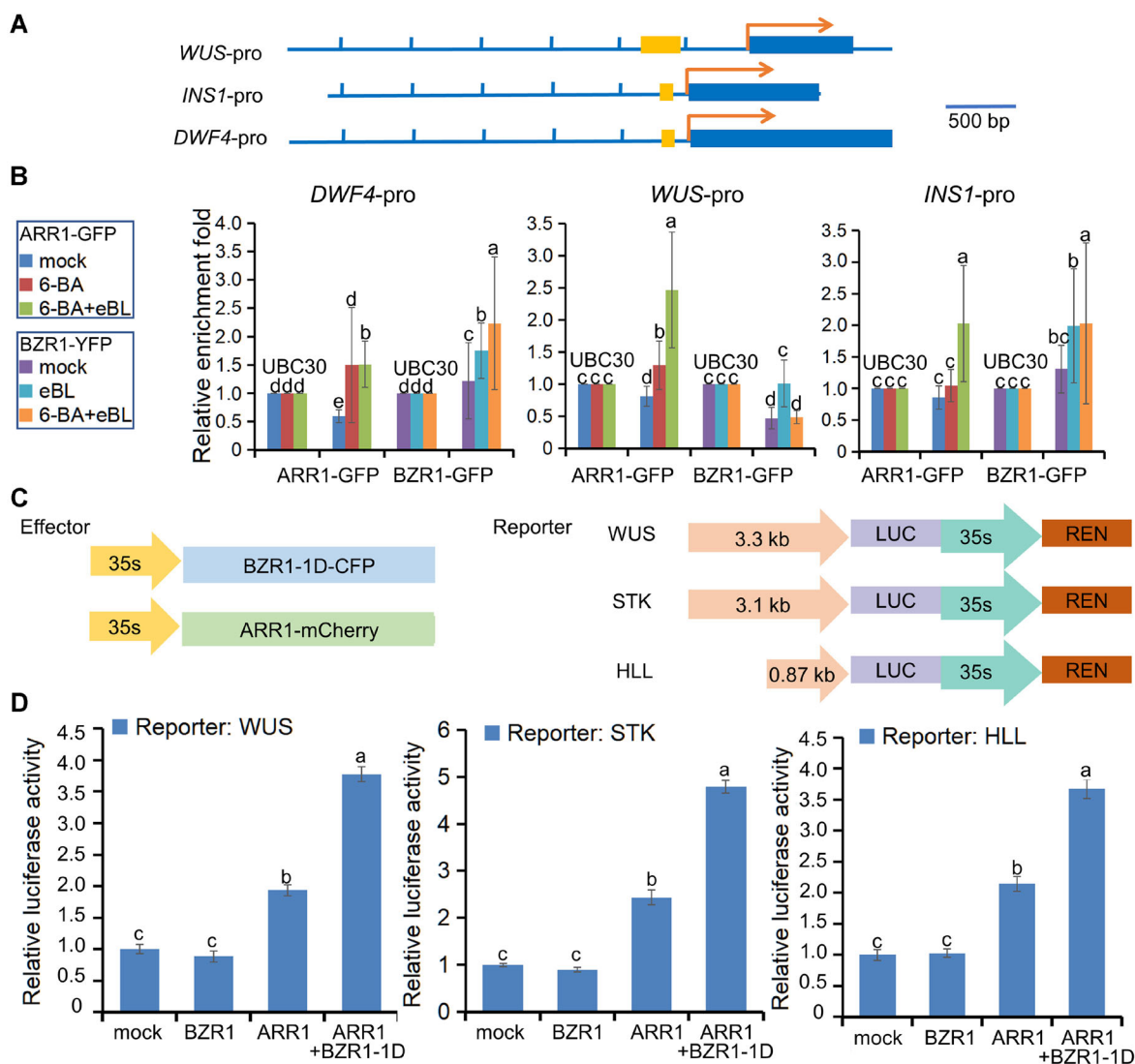
Figure 6. BRASSINAZOLE-RESISTANT 1 (BZR1) enhances the ability of REGULATOR1 (ARR1) to transcriptionally regulate downstream genes to influence ovule initiation and seed number per silique (SNS)

(**A**) Genomic sequences of *WUS*, *INS1*, and *DWF4*. Blue lines and boxes indicate promoter and coding regions, respectively. Yellow box marks promoter regions (*WUS*: −770 bp to −533 bp; *INS1*:−198 bp to −99 bp; *DWF4*:−743 bp to −601 bp) used in chromatin immunoprecipitation (ChIP) analyses. (**B**) ChIP analyses using pARR1:ARR1-GFP and pBZR1:BZR1-YFP. Seedlings (7 d after germination) treated with 30 min 1 μmol/L eBL or 1 μmol/L 6-BA were used for ChIP analyses. Immunoprecipitation was conducted with anti-GFP beads. Error bars represent *SE* (*n* = 3 biological replicates). Lowercase letters indicate statistically significant differences between different stages (*P* < 0.05). (**C**) Diagrams of the effector and reporter constructs used in (**D**) (*WUS*: −3301 bp to −533 bp; *STK*: −2,008 bp to 1,085 bp; *HLL*: −878 bp to 0 bp). (**D**) Transient activation assays in tobacco leaves. Bars represent mean ± *SD* of three biological replicates (*n* = 30). Lowercase letters indicate statistically significant differences between different stages (*P* < 0.05).

and *bzr1-1D*, with the *35S:CKX3* lines that showed significantly increased *CKX3* expression (Figure S4C). There were no significant differences of SNS between the *35S:CKX3 DWF4-OX* or *35S:CKX3 bzr1-1D* lines and *35S:CKX3* plants (Figure 7C). The increased BR signaling in an *arr1 bzr1-1D* line did not restore the decreased SNS of the *arr1* mutant (Figure S4D). These results revealed that increased BR signaling does not rescue the CK-reduced phenotypes of poor growth (Figure 7B) and decreased SNS (Figures 7C, S4D).

Overall, our results indicated that BR regulates the SNS through strengthening CK function. Since BR and CK increased

the SNS in a coordinate manner, and enhanced CK only partially rescued BR-reduced mutants, BR likely regulates the SNS via CK-dependent and -independent pathways (Figure 7D).

DISCUSSION

BR and CK interaction promoted ovule initiation and increased the SNS

Previous studies demonstrated that BR and CK positively regulate plant growth and seed number, indicating that they
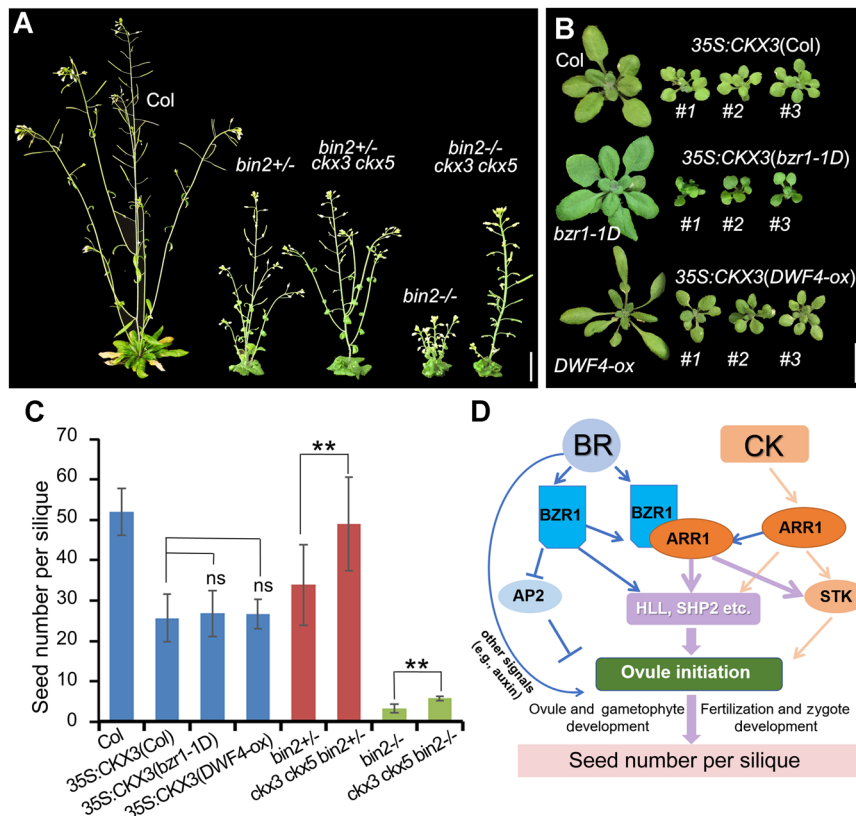
Figure 7. Brassinosteroid (BR) regulates seed number per silique (SNS) partially through a cytokinin (CK)-mediated pathway

Adult plants (50 d after germination: DAG) of wild type (Col), $bin2^{+/-}$, $bin2^{+/-}ckx3\ ckx5$, $bin2^{-/-}$, and $bin2^{-/-}ckx3\ ckx5$ (scale bars, 2 cm). (**B**) Seedlings (30 DAG) of Col, *35S:CKX3-GFP*, *bzr1-1D*, *bzr1-1D 35S:CKX3-GFP*, *DWF4-ox*, and *DWF4-ox 35S:CKX3-GFP* (scale bars, 2 cm). (**C**) Statistical analysis of seed number per silique (SNS) of above lines. Bars represent mean ± *SD* of three biological replicates (*n* = 30). Asterisks indicate significant difference (Student's two-tailed *t*-test: *$P < 0.05$; **$P < 0.01$). (**D**) Hypothetical model of how BZR1 and ARR1 cooperate to regulate ovule initiation and SNS in *Arabidopsis*. CK regulates ovule initiation through transcriptional regulation of downstream genes involved in ovule initiation (e.g., *STK*, *HLL*, and *SHP2*) via the CK-response transcription factor ARR1. In this model, the blue/orange arrows and lines represent the pathways of BR/CK, respectively, and the purple arrows and lines represents how the pathways cooperate to regulate by two hormones. BR regulates ovule initiation through transcriptional regulation of downstream genes involved in ovule initiation (e.g., *AP2*, *HLL*, and *SHP2*) via the BR-induced transcription factor, BZR1. BR enhances CK function through strengthening the interaction between BZR1 and ARR1, thereby strengthening ARR1 ability of transcriptional regulation of downstream genes (e.g., *STK* and *HLL*), thus promoting ovule initiation and SNS in *Arabidopsis*. BR also positive regulate ovule initiation through other ways, for example, enhancing auxin response.

contribute to seed yield by increasing seed number (Higuchi et al., 2004; Bartrina et al., 2011; Huang et al., 2013; Jiang et al., 2013). Therefore, we infer that ovule number is likely increased in BR- and CK-enhanced mutants. Conversely, mutants that are deficient in or insensitive to BR and CK show arrested growth, smaller flowers, and reduced SNS. The regulatory mechanisms of these two hormones in ovule initiation may differ since BR is mainly involved in cell elongation while CK generally promotes cell division (Sakakibara, 2006; Zhang et al., 2009, 2013; Tong et al., 2014). The BR-enhanced mutant *bzr1-1D* and the CK-enhanced mutant *ckx3 ckx5* show increased SNS. Our detailed phenotypic analysis demonstrated that these mutants exhibit enlarged siliques and increased ovule number, but with normal gametophyte development, fertilization, and zygote development, which leads to increased SNS. Both mutants show increased pistil, placenta, and silique lengths, which can result in increased ovule

initiation. The *ckx3 ckx5 bzr1-1D* triple mutant had a longer placenta and more ovules than the *bzr1-1D* mutant, and a similar placenta length with more ovules than the *ckx3 ckx5* mutant (Figure 1F, G). This suggests that CK may improve ovule initiation by increasing space in the placenta for more ovules, and BR promotes ovule initiation through other mechanisms, and both signals coordinate to promote ovule initiation and SNS. Based on the results that enhanced CK signaling partially rescued the SNS phenotypes of BR-deficient or -insensitive mutants (Figure 7A–C), we speculate that CK is required for BR-promoted seed number. Taken together, BR and CK do not function entirely in the same pathway but they overlap and coordinate to promote ovule initiation (Figure 7D).

Here, we present several lines of evidence that BR and CK jointly regulate ovule initiation. The qRT-PCR analyses, in which BR induced the expression of CK-positive marker genes (Figures 2A, 3A) while CK repressed the expression of

BR-negative marker genes, suggest that BR positively regulates the CK response and that CK enhances the BR signal. This was supported by GFP observations and western blot assays. Based on GFP fluorescence, BR induced the activity and abundance of *TCS:GFP*, and thus the CK response (Figures 2B, C, S2). Based on the western blot analyses, TCS:GFP protein abundance was increased in the *bzr1-1D* background but decreased in the *bin2* background, again demonstrating that BR upregulates the CK signal (Figure 2D). Furthermore, the increased BZR1 protein level (Figure 3C) and enhanced BZR1-YFP signals in the nucleus in the CK-enhanced mutant (Figure 3B) imply that CK positively regulates BR signaling. Finally, the triple mutant with enhanced BR and CK signaling showed increased transcription of several ovule initiation genes, suggesting that BR and CK promote ovule initiation through coregulating ovule initiation genes (*STK* and *HLL*, suggested by the LUC assay, Figure 6D).

Enhanced CK signaling partially rescued the ovule and SNS phenotypes of BR-deficient or -insensitive mutants (Figures 7, S4B), which indicated that BR regulates the SNS partially through a CK-dependent manner. Our finding that enhanced BR signaling did not rescue the reduced SNS phenotype in CK-deficient plants, but increased the SNS phenotype in the CK-enhanced mutant (Figure 7), suggested that BR also regulates the SNS via a CK-independent pathway (Figure 7D). Our previous study demonstrated that BR positively regulates ovule initiation through enhancing the auxin response and direct transcriptional regulation of downstream genes involved in early ovule development. Here, we clarified that some ovule initiation regulators (e.g., *AP2*) are specifically regulated by BR, some are directly regulated by CK (e.g., *STK*; BR strengthened CK function), and some (e.g., *HLL*, *SHP1/2*, and *ANT*) are regulated by both BR and CK. Therefore, simultaneously enhancing BR and CK signaling induces genes regulated by BR and CK, as well as the CK-mediated regulators of ovule initiation, thereby promoting ovule initiation and increasing the SNS (Figure 7D). The new candidate genes identified by our transcriptomic analysis warrant further investigation to find more genes involved in BR- and/or CK-mediated regulation of ovule initiation.

Newly identified candidate genes that promote ovule initiation and increase the SNS

We identified many candidate downstream genes by transcriptomic comparisons among *ckx3 ckx5*, *bzr1-1D*, and *ckx3 ckx5 bzr1-1D* mutants. We isolated young pistils of floral stage 8 with empty placentae to avoid influencing the transcriptome analysis. Stigmas and junctions of floral organs were removed to exclude interference. The set of DEGs included some known genes, such as three D class genes of the ABCDE model (*STK* and *SHP1/2*) that are involved in development of the placenta from the carpel margin meristem and early ovule development (Villarino et al., 2016). Other known genes included the transcription factor *ANT*, regulators *HLL* and *AGL* (Sun et al., 2010; Schmidt et al., 2011; Chen et al., 2012), and several hormone-related genes (Paponova et al., 2008; Sun et al., 2010; Schmidt et al., 2011).

The expression of marker genes *CPD*, *DWF4*, and *ARR5/7/15* was altered in the BR- or CK-related mutants. The expression of candidate genes *STK*, *HLL*, and *SHP2* demonstrated that BR and CK regulate ovule initiation by inducing the positive regulators of ovule identity and initiation (Figure 5F). In addition, our data suggested that BR and CK increase ovule initiation by coordinately inducing the expression of positive regulators such as *SHP1* and *ANT* (Figure S1). These experiments demonstrated that BR and CK regulate ovule initiation through affecting the expression of genes involved in ovule initiation.

We detected 18 genes that were upregulated and 189 genes that were downregulated in *bzr1-1D* and *ckx3 ckx5* mutants. As shown in Figure 5, there was almost no overlap between the BR-upregulated genes and the CK-downregulated genes, or between the CK-upregulated genes and the BR-downregulated genes (Figure 5). This suggested that BR and CK function coordinately to regulate the SNS. A few genes were upregulated in all three mutants (*ckx3 ckx5*, *bzr1-1D*, and *ckx3 ckx5 bzr1-1D*), suggesting that BR and CK share a gene network to promote ovule initiation. The finding that several genes encoding metabolic enzymes were downregulated in *ckx3 ckx5*, *bzr1-1D*, and *ckx3 ckx5 bzr1-1D* suggested that BR and CK likely suppress some primary metabolic pathways to conserve energy for cell division and expansion in the placenta, resulting in enlarged placentae and more ovule primordia.

Interaction of BR and CK signaling pathways in ovule initiation and SNS

This work demonstrates that the cross-talk between BR and CK plays important roles in ovule initiation and SNS. BZR1 directly interacted with ARR1, and treatment with BR and co-treatment with BR and CK enhanced the interaction between these two transcription factors, further indicating that enhanced BR signaling increased their effect on ovule initiation via regulation of common and specific target genes. The qRT-PCR and ChIP analyses demonstrated that downstream genes were targeted by BZR1 and/or ARR1, and that enhanced BR and CK signaling strengthened this targeting. Consequently, BR and/or CK further induced or repressed these genes to regulate the SNS. ARR1 induced *WUS* expression (Zhang et al., 2017). *STK* and *HLL*, two ovule initiation genes, were induced by ARR1, and enhanced BZR1 activity strengthened the ARR1-mediated induction of *STK*, *HLL*, and *WUS* (Figure 6), suggesting that BR positively regulates ovule initiation and development through strengthening CK signaling (Figure 7D). Furthermore, we conclude that BR regulates the SNS through a CK-mediated pathway.

INS1, a newly identified gene, was strongly targeted by BZR1 but not significantly targeted by ARR1. Treatment with BR strengthened the targeting of *INS1* by ARR1, while treatment with CK did not strengthen the targeting of *INS1* by BZR1, suggesting that *INS1* regulation is BR specific and that BR might also regulate the SNS through a CK-independent pathway. Our results showed that BR regulates genes involved in ovule initiation and SNS through CK-mediated and -independent pathways by strengthening the interaction between BZR1 and ARR1.

The candidate genes identified here have potential application in increasing the seed yield of dicot crops.

MATERIALS AND METHODS

Plant materials, growth conditions, and transformation procedure

All *Arabidopsis* plant materials were in the Col-0 ecotype background. The *arr1* (CS6971), *arr10* (CS39989), *arr12* (CS6978), *arr1 arr10* (CS39990), *arr1 arr12* (CS6981), and *arr1 arr10 arr12* (CS39992) mutants and *TCS:GFP* transgenic lines were provided by the Arabidopsis Biological Resource Center. The double mutant *ckx3 ckx5* was obtained by crossing *ckx3* (SALK_050938) with *ckx5* (SALK_064309). The triple mutant *ckx3 ckx5 bzr1-1D* was obtained by crossing *ckx3 ckx5* with *bzr1-1D*. Because the vegetative growth and fertility of homozygous mutants of *bin2* are very poor, the experiments involving the *bin2* mutant in this experiment used both homozygous mutants ($bin2^{-/-}$) and heterozygous mutants ($bin2^{+/-}$) of *bin2* (Li et al., 2001). The triple mutants *ckx3 ckx5 bin2$^{+/-}$* and *ckx3 ckx5 bin2$^{-/-}$* were obtained by crossing *ckx3 ckx5* with $bin2^{+/-}$ and $bin2^{-/-}$, respectively. The triple mutant *ckx3 ckx5 det2* was obtained by crossing *ckx3 ckx5* with *det2*. The *bzr1-1D TCS:GFP* line was obtained by *bzr1-1D* with *TCS:GFP*, and the *bin2$^{+/-}$TCS:GFP* line was obtained by crossing *bin2$^{+/-}$* with *TCS:GFP*.

All *Arabidopsis* plants were grown in soil under glass-house conditions (22°C; 16-h light: 8-h dark photoperiod for long-day conditions) or on half- strength Murashige and Skoog (½ MS) medium (Murashige and Skoog,1962) containing 2% (w/v) sucrose and 0.75% (w/v) agar in a growth chamber (22°C:18°C, 16-h light: 8-h dark photoperiod). The *35S:CKX3-GFP* (pCAMBIA1302) vector was transformed into wild type (WT) *Arabidopsis* plants (Col-0), *bzr1-1D*, and *DWF4-ox*. *Agrobacterium*-mediated transformation was performed using the floral-dip method (Clough and Bent, 1998).

Hormone and inhibitor treatments in culture systems

Flowers were submerged in the medium. In the pistil culture method, hormone and inhibitor solution was dropped directly onto a single excised pistil with a pipette as described in a previous paper (Li et al., 2018). The pistils were immersed in, and slowly absorbed, the phytohormone solution. The 6-BA and eBL was dissolved in ethanol to a stock concentration of 10 mmol/L; mock treatments were performed with distilled water containing 0.2% (v/v) ethanol and 0.01% SilwetL-77. The hormone treatments used in this article are all short-term, high-concentration treatments (30 min 1 μmol/L eBL and 30 min 1 μmol/L BRZ).

Construction of vectors

The 1,570-bp coding sequence (CDS) of *CKX3* was amplified by PCR with KOD-FX DNA polymerase and the primers 35:CKX3-GFP-F and 35:CKX3-GFP-R, and then cloned into the pCAMBIA1302 vector (digested with EcoRI and NcoI) to generate the 35S:CKX3-GFP vector. The 1,008-bp CDS of

BZR1 was amplified by PCR with KOD-FX DNA polymerase and the primers pGBKT7-BZR1-F and pGBKT7-BZR1-R, and then cloned into the pGBKT7 vector (digested with NdeI and BamHI) to generate the pGBKT7-BZR1 vector. Similarly, the CDS of *BZR1* was amplified using the primers pXY104-BZR1-F and pXY104-BZR1-R, and cloned into the pXY104 vector (digested with SpeI) to generate the pMY304-BZR1 vector; and with the primers pGEX-4T-1-BZR1-F and pGEX-4T-1-BZR1-R, and cloned into the pGEX-4T vector (digested with EcoRI) to generate the pGEX-4T-1-BZR1 vector. The 2,070-bp CDS of *ARR1* was amplified by PCR with KOD-FX DNA polymerase and the primers pGADT7-ARR1-F and pGADT7-ARR1-R, and cloned into the pGADT7 vector (digested with NdeI and BamHI) to generate the pGADT7-ARR1 vector. Similarly, the *ARR1* CDS was amplified with the primers pXY104-ARR1-F and pXY104-ARR1-R, and cloned into the pXY104 vector (digested with SpeI) to generate the pXY104-ARR1 vector; and with the primers pET30a$^+$-HIS-ARR1-F and pET30a$^+$-HIS-ARR1-R, and cloned into the pET30a$^+$ vector (digested with BamHI) to generate the pGEX-4T-1-BZR1 vector. All primer sequences are shown in Table S1.

qRT-PCR assays

Quantitative real-time PCR assays were carried out as described previously (Zhang et al., 2016). Primer sequences are shown in Table S1. For each experiment, three biological replicates were analyzed.

Confocal imaging analysis

Roots for fluorescence observation were separated from seedlings (5 d after germination: DAG), which were grown vertically in ½ MS medium containing 2% (w/v) sucrose. Ovules were separated from pistils of flowers at developmental stages 10 and 11, and fixed, cleaned, and dyed. For confocal fluorescence microscopy, after the pistil side was slit open, it was fixed in 4% paraformaldehyde for half an hour, and then soaked in Clearsee solution for a week as described before (Kurihara et al., 2015). Before observation, dissolve calcofluor white (Fluorescent brightener 28) in Clearsee solution was used to stain the cell wall of the ovule. For observation, the ovule was sealed with Clearsee solution and observed with an Upright Laser Confocal Microscope (Nikon & Nikon Ni-E A1 HD25). The excitation and emission wavelengths were as follows: calcofluor white, excitation at 405 nm and emission at 425–475 nm; CFP, excitation at 445 nm and emission at 455–505 nm; GFP and YFP, excitation at 488 nm and emission at 505–550 nm; and FM4-64 and mCherry, excitation at 561 nm and emission at 575–620 nm. All samples were observed using the same parameters: confocal pinhole, 1.2 μm; excitation intensity, 15; HV, 30. Details of these methods are described elsewhere (Jiang et al., 2020).

Identification and characterization of transgenic lines

The *35S:CKX3-GFP* transgenic lines were verified with primers 35S:CKX3-GFP-F4 and GFP. Primer sequences are shown in Table S1. The phenotype of 21 d old plants and the leaf shape of transgenic lines were photographed using a

Canon EOS60D digital camera. The siliques from different lines were observed under a Leica S8APO stereomicroscope and photographed with a Leica DFC450 digital camera. Three biological replicates were analyzed for each line. Silique length was analyzed using IMAGEJ software (http://rsbweb. nih.gov/ij/download.html).

Bimolecular fluorescence complementation assays

The CDSs of *BZR1* and *ARR1* were amplified and cloned into the pXY106-nYFP and pXY104-cYFP plasmids. The recombinant vectors were co-transformed into *Agrobacterium tumefaciens* GV3101. After collection by centrifugation, the bacterial cells were resuspended in infection solution (10 mmol/L MES, 10 mmol/L MgCl$_2$, and 200 μmol/L acetosyringone) to OD$_{600}$ = 0.6 for infiltration. The prepared suspensions were infiltrated into *Nicotiana benthamiana* leaves and the plants were kept in the dark for 2 d. Fluorescent YFP signals were monitored under a Leica SP8 confocal microscope.

Western blot assays

Protein extraction and immunoblots were performed as described previously (Wang et al., 2020). The antibodies used in this study were anti-GFP, anti-mCherry, anti-BZR1, anti-TUBULIN A, anti-ACTIN, anti-HIS, and anti-GST. The quantifications of the western blots were made using ImageJ (https://imagej.nih.gov/ij/). In each related experiment, the number of repeats (n) and statistical methods are indicated in the figure legends.

Yeast two-hybrid assay

The CDSs of *BZR1* and truncated or mutated *ARR1* were amplified and cloned into pGBKT7 or pGADT7 (Clontech) and then transformed into the yeast stain AH109. Yeast transformants were plated onto minimal SD Agar Base (Clontech) plates supplemented with DO Supplement -Leu/-Trp (Clontech) and further incubated for 4 d at 30°C. Finally, well-grown colonies were plated onto minimal SD Agar Base (Clontech) plates supplemented with DO Supplement -His/-Leu/-Trp/-Ade (Clontech) for activity assays.

In vitro pull-down assays

The full-length CDSs of *BZR1* and *ARR1* were each cloned into pGEX-4T-1 and pET30a+ to generate BZR1-GST and ARR1-HIS. These proteins were expressed in, and purified from, *E. coli* BL21. Anti-GST antibodies were used to pull-down the protein complexes, and unbound proteins were removed by washing. The bound proteins were eluted and analyzed by immunoblotting with an anti-His antibody. GST-BZR1 was incubated with the HIS-ARR1 and GST beads were used to pull-down the protein complexes. The proteins were eluted and analyzed by immunoblotting with anti-HIS or anti-GST antibodies.

In vitro co-immunoprecipitation assays

Proteins were extracted from tobacco epidermal cells co-expressing ARR1-mcherry and BZR1-GFP, which were ground in liquid nitrogen to a fine powder. Protein Immunoprecipitation was conducted as described previously with the GFP antibody. mCherry-tagged ARR1 and GFP-tagged BZR1 were detected by western blotting using the GFP antibody and the mCherry antibody.

Chromatin immunoprecipitation assays

According to a published protocol (Wang et al., 2020), 7 DAG seedlings of Col expressing *pARR1:ARR1-GFP* were prepared for analyses after 2 h treatment with 100 nmol/L eBL or 2 h treatment with 10 μmol/L 6-BA. The chromatin extract was immunoprecipitated with anti-GFP beads. All primer sequences are shown in Table S1. For all of the ChIP experiments, three biological replicates were analyzed.

Dual LUC assay

According to a published protocol (Wang et al., 2020), the effector and reporter vectors were co-transformed into *A. tumefaciens* GV3101 and were infiltrated into *N. benthamiana* leaves and the plants were kept in the dark for 2 d. LUC and REN activities were quantified and measured with a luminometer (Promega 20/20). LUC activity was calculated by normalizing to that of REN. Three independent experiments (biological triplicates) were performed.

CONFLICTS OF INTEREST

The authors declare that there is no conflicts of interest.

AUTHOR CONTRIBUTIONS

W.H.L. designed the study, analyzed data, organized results, wrote and modified the manuscript, and acquired funding.

S.H.Z. and Y.T.J. performed experiments, analyzed data, organized results, and wrote the manuscript. J.H.C. and Y.J.Z. helped performed experiments. H.W.X. helped edit the manuscript. All authors agree to be accountable for the content of this paper.

REFERENCES

Bartrina, I., Otto, E., Strnad, M., Werner, T., and Schmulling, T. (2011). Cytokinin regulates the activity of reproductive meristems, flower organ size, ovule formation, and thus seed yield in *Arabidopsis thaliana*. Plant Cell **23:** 69–80.

Chaudhury, A.M., Ming, L., Miller, C., Craig, S., Dennis, E.S., and Peacock, W.J. (1997). Fertilization-independent seed development in *Arabidopsis thaliana*. Proc. Natl. Acad. Sci. U.S.A. **94:** 4223–4228.

Chen, C.C., Fu, S.F., Lee, Y.I., Lin, C.Y., Lin, W.C., and Huang, H.J. (2012). Transcriptome analysis of age-related gain of callus-forming capacity in *Arabidopsis* hypocotyls. Plant Cell Physiol. **53:** 1457–1469.

Clough, S.J., and Bent, A.F. (1998). Floral dip: A simplified method for *Agrobacterium* mediated transformation of *Arabidopsis thaliana*. Plant J. **16:** 735–743.

Clouse, S.D., Langford, M., and McMorris, T.C. (1996). A brassinosteroid-insensitive mutant in *Arabidopsis thaliana* exhibits multiple defects in growth and development. Plant Physiol. **111:** 671–678.

Clouse, S.D., and Sasse, J.M. (1998). BRASSINOSTEROIDS: Essential regulators of plant growth and development. Annu. Rev. Plant Physiol. Plant Mol. Biol. **49:** 427–451.

Cucinotta, M., Colombo, L., and Roig-Villanova, I. (2014). Ovule development, a new model for lateral organ formation. Front. Plant Sci. **5:** 117.

Favaro, R., Pinyopich, A., Battaglia, R., Kooiker, M., and Borghi, L. (2003). MADS-Box protein complexes control carpel and ovule development in *Arabidopsis*. Plant Cell **15:** 2603–2611.

Ferreira, F.J., and Kieber, J.J. (2005). Cytokinin signaling. Curr. Opin. Plant Biol. **8:** 518–525.

Fujioka, S., and Yokota, T. (2003). Biosynthesis and metabolism of brassinosteroids. Annu. Rev. Plant Biol. **54:** 137–164.

Galbiati, F., Sinha Roy, D., Simonini, S., Cucinotta, M., Ceccato, L., Cuesta, C., Simaskova, M., Benkova, E., Kamiuchi, Y., Aida, M., Weijers, D., Simon, R., Masiero, S., and Colombo, L. (2013). An integrative model of the control of ovule primordia formation. Plant J. **76:** 446–455.

Gambín, B.L., and Borrás, L. (2010). Resource distribution and the trade-off between seed number and seed weight: A comparison across crop species. Ann. Appl. Biol. **156:** 91–102.

Groß-Hardt, R., Lenhard, M., and Laux, T. (2002). WUSCHEL signaling functions in interregional communication during *Arabidopsis* ovule development. Genes Dev. **16:** 1129–1138.

Grove, M.D., Spencer, G.F., Rohwedder, W.K., Mandava, N., and Cook, J.L.C. (1979). Brassinolide, a plant growth-promoting steroid isolated from *Brassica napus* pollen. Nature **281:** 216–217.

He, J.X., Gendron, J.M., Sun, Y., Gampala, S.S.L., Gendron, C.N., Sun, Q., and Wang, Z.Y. (2005). BZR1 Is a transcriptional repressor with dual roles in brassinosteroid homeostasis and growth responses. Science **307:** 1634–1638.

He, J.X., Gendron, J.M., Yang, Y., Li, J., and Wang, Z.Y. (2002). The GSK3-like kinase BIN2 phosphorylates and destabilizes BZR1, a positive regulator of the brassinosteroid signaling pathway in *Arabidopsis*. Proc. Natl. Acad. Sci. U.S.A. **99:** 10185–10190.

Higuchi, M., Pischke, M.S., AP, M., Miyawaki, K., Hashimoto, Y., and Seki, M. (2004). In planta functions of the *Arabidopsis* cytokinin receptor family. Proc. Natl. Acad. Sci. U.S.A. **101:** 8821–8826.

Huang, H.Y., Jiang, W.B., Hu, Y.W., and Wu, P. (2013). BR signal influences *Arabidopsis* ovule and seed number through regulating related genes expression by BZR1. Mol. Plant **6:** 456–469.

Jennifer, P.C.,T., Haberer, G., Ferreira, F.J., Deruère, J., Mason, M.G., Schaller, G.E., Alonso, J.M., Ecker, J.R., and Kieber, J.J. (2004). Type-A *Arabidopsis* response regulators are partially redundant negative regulators of cytokinin signaling. Plant Cell **16:** 658–671.

Jiang, H.F., and Egli, D.B. (1995). Soybean seed number and crop growth rate during flowering. Agron. J. **87:** 264–267.

Jiang, W.B., Huang, H.Y., Hu, Y.W., and Zhu, S.W. (2013). Brassinosteroid regulates seed size and shape in *Arabidopsis*. Plant Physiol. **162:** 1965–1977.

Jiang, Y.T., Tang, R.J., Zhang, Y.J., Xue, H.W., Ferjani, A., Luan, S., and Lin, W.H. (2020). Two tonoplast proton pumps function in *Arabidopsis* embryo development. New Phytol. **225:** 1606–1617.

Kiniry, J.R., Wood, C.A., Spanel, D.A., and Bockholt, A.J. (1990). Seed weight response to decreased seed number in maize. Agron. J. **82:** 98–102.

Kurihara, D., Mizuta, Y., Sato, Y., and Higashiyama, T. (2015). ClearSee: A rapid optical clearing reagent for whole-plant fluorescence imaging. Development **142:** 4168–4179.

Li, B.F., Yu, S.X., Hu, L.Q., Zhang, Y.J., Zhai, N., Xu, L., and Lin, W.H. (2018). Simple culture methods and treatment to study hormonal regulation of ovule development. Front. Plant Sci. **9:** 784.

Li, J., Nam, K.H., Vafeados, D., and Chory, J. (2001). BIN2, a new brassinosteroid-insensitive locus in *Arabidopsis*. Plant Physiol. **127:** 14–22.

Liu, X.B., Herbert, S.J., Zhang, Q.Y., and Hashemi, A.M. (2006). Yield–density relation of glyphosate-resistant soya beans and their responses to light enrichment in north-eastern USA. J. Agron. Crop Sci. **193:** 55–62.

Liu, Z., Yuan, L., Song, X., Yu, X., and Sundaresan, V. (2017). AHP2, AHP3, and AHP5 act downstream of CKI1 in *Arabidopsis* female gametophyte development. J. Exp. Bot. **68:** 3365–3373.

Mason, M.G., Mathews, D.E., Argyros, D.A., Maxwell, B.B., Kieber, J.J., Alonso, J.M., Ecker, J.R., and Schaller, G.E. (2005). Multiple type-B response regulators mediate cytokinin signal transduction in *Arabidopsis*. Plant Cell **17:** 3007–3018.

Mizuno, T. (2005). Two-component phosphorelay signal transduction systems in plants: From hormone responses to circadian rhythms. Biosci. Biotechnol. Biochem. **69:** 2263–2276.

Monpara, B.A., and Gaikwad, S.R. (2014). Combining high seed number and weight to improve seed yield potentian of chickpea in India. Afr. Crop Sci. J. **22:** 1–7.

Morris, R.O., Bilyeu, K.D., Laskey, J.G., and Cheikh, N.N. (1999). Isolation of a gene encoding a glycosylated cytokinin oxidase from maize. Biochem. Biophys. Res. Commun. **255:** 328–333.

Murashige, T., and Skoog, F. (1962). A revised medium for rapid growth and bioassays with tobacco tissue culture. Physiol. Plant. **15:** 473–479.

Ohnishi, T., Godza, B., Watanabe, B., Fujioka, S., Hategan, L., Ide, K., Shibata, K., Yokota, T., Szekeres, M., and Mizutani, M. (2012). CYP90A1/CPD, a brassinosteroid biosynthetic cytochrome P450 of *Arabidopsis*, catalyzes C-3 oxidation. J. Biol. Chem. **287:** 31551–31560.

Paponova, I.A., Paponova, M., Tealea, W., Mengesb, M., Chakraborteeb, S., Murrayb, J.A.H., and Palmea, K. (2008). Comprehensive

transcriptome analysis of auxin responses in *Arabidopsis*. Mol. Plant **1**: 321–337.

Purohit, S.S. (1985). *Hormonal Regulation of Plant Growth and Development*. India: Dordrecht and Agro Botanical Publishers.

Rin, H.H., Pethe, C., and D'Alayer, J. (2002). Cytokinin oxidase from *Zea mays*: Purification, cDNA cloning and expression in moss protoplasts. Plant J. **17**: 615–626.

Sakakibara, H. (2006). Cytokinins: Activity, biosynthesis, and translocation. Annu. Rev. Plant Biol. **57**: 431–449.

Schmidt, A., Wuest, S.E., Vijverberg, K., Baroux, C., Kleen, D., and Grossniklaus, U. (2011). Transcriptome analysis of the *Arabidopsis* megaspore mother cell uncovers the importance of RNA helicases for plant germline development. PLoS Biol. **9**: e1001155.

Schneitz, K., Baker, S.C., Gasser, C.S., and Redweik, A. (1998). Pattern formation and growth during floral organogenesis: HUEL-LENLOS and AINTEGUMENTA are required for the formation of the proximal region of the ovule primordium in *Arabidopsis thaliana*. Development **125**: 2555.

Schou, J.B., Jeffers, D.L., and Streeter, J.G. (1978). Effects of reflectors, black boards, or shades applied at different stages of plant development on yield of soybeans. Crop Sci. **18**: 29–34.

Song, X.J., Huang, W., Shi, M., Zhu, M.Z., and Lin, H.X. (2007). A QTL for rice grain width and weight encodes a previously unknown RING-type E3 ubiquitin ligase. Nat. Genet. **39**: 623–630.

Sun, Y., Fan, X.Y., Cao, D.M., Tang, W., He, K., Zhu, J.Y., He, J.X., and Wang, Z.Y. (2010). Integration of brassinosteroid signal transduction with the transcription network for plant growth regulation in *Arabidopsis*. Dev. Cell **19**: 777.

Takatoshi, K., Hisami, Y., Shusei, S., Tomohiko, K., Satoshi, T., Takafumi, Y., and Takeshi, M. (2003). The type-A response regulator, ARR15, acts as a negative regulator in the cytokinin-mediated signal transduction in *Arabidopsis thaliana*. Plant Cell Physiol. **44**: 868–874.

Tong, H., Xiao, Y., Liu, D., Gao, S., Liu, L., Yin, Y., Jin, Y., Qian, Q., and Chu, C. (2014). Brassinosteroid regulates cell elongation by modulating gibberellin metabolism in rice. Plant Cell **26**: 4376.

Villarino, G.H., Hu, Q., Manrique, S., Flores-Vergara, M., Sehra, B., Robles, L., Brumos, J., Stepanova, A.N., Colombo, L., Sundberg, E., Heber, S., and Franks, R.G. (2016). Transcriptomic signature of the SHATTERPROOF2 expression domain reveals the meristematic nature of *Arabidopsis* gynoecial medial domain. Plant Physiol. **171**: 42–61.

Wang, L., Wang, B., Yu, H., Guo, H., Lin, T., Kou, L., Wang, A., Shao, N., Ma, H., Xiong, G., Li, X., Yang, J., Chu, J., and Li, J. (2020). Transcriptional regulation of strigolactone signalling in *Arabidopsis*. Nature **583**: 277–281.

Wang, Z.Y., Bai, M.Y., Oh, E., and Zhu, J.Y. (2012). Brassinosteroid signaling network and regulation of photomorphogenesis. Annu. Rev. Genet. **46**: 701–724.

Wang, Z.Y., Nakano, T., Gendron, J., He, J., Chen, M., Vafeados, D., Yang, Y., Fujioka, S., and Chory, J. (2002). Nuclear-localized BZR1 mediates brassinosteroid-induced growth and feedback suppression of brassinosteroid biosynthesis. Dev. Cell **2**: 505–513.

Weigel, D., and Meyerowitz, E. (1994). The ABCs of floral homeotic genes. Cell **78**: 203–209.

Xie, M., Chen, H., Huang, L., O'Neil, R.C., Shokhirev, M.N., and Ecker, J.R. (2018). A B-ARR-mediated cytokinin transcriptional network directs hormone crossregulation and shoot development. Nat. Commun. **9**: 1604.

Yu, S.X., Zhou, L.W., Hu, L.Q., Jiang, Y.T., Zhang, Y.J., Feng, S.L., Jiao, Y., Xu, L., and Lin, W.H. (2020). Asynchrony of ovule primordia initiation in *Arabidopsis*. Development **147**: dev196618

Zhang, L.Y., Bai, M.Y., Wu, J., Zhu, J.Y., Wang, H., Zhang, Z., Wang, W., Sun, Y., Zhao, J., and Sun, X. (2009). Antagonistic HLH/bHLH transcription factors mediate brassinosteroid regulation of cell elongation and plant development in rice and *Arabidopsis*. Plant Cell **21**: 3767–3780.

Zhang, T.Q., Lian, H., Zhou, C.M., Xu, L., Jiao, Y., and Wang, J.W. (2017). A two-step model for de novo activation of WUSCHEL during plant shoot regeneration. Plant Cell **29**: 1073–1087.

Zhang, Y., Li, B., Xu, Y., Li, H., Li, S., Zhang, D., Mao, Z., Guo, S., Yang, C., and Weng, Y. (2013). The cyclophilin CYP20-2 modulates the conformation of BRASSINAZOLE-RESISTANT1, which binds the promoter of *FLOWERING LOCUS D* to regulate flowering in *Arabidopsis*. Plant Cell **25**: 2504–2521.

Zhang, Y., Zhang, Y.J., Yang, B.J., Yu, X.X., Wang, D., Zu, S.H., Xue, H.W., and Lin, W.H. (2016). Functional characterization of GmBZL2 (AtBZR1 like gene) reveals the conserved BR signaling regulation in *Glycine max*. Sci. Rep. **6**: 31134.

SUPPORTING INFORMATION

Additional Supporting Information may be found online in the supporting information tab for this article: http://onlinelibrary.wiley.com/doi/10.1111/jipb.13197/suppinfo

Dataset S1. Differentially expressed genes (DEGs) of *bzr1-1D* vs Col, *ckx3 ckx5* vs Col, and *ckx3 ckx5 bzr1-1D* vs Col
Figure S1. Cytokinin (CK) and brassinosteroid (BR) regulate ovule initiation

(**A**) Statistical analysis of seed number per silique of ARR loss-of-function mutants. Bars represent mean ± SD of three biological replicates (*n* = 15). Asterisks indicate significant difference (Student's two-tailed *t*-test: *P < 0.05; **P < 0.01). Quantitative reverse transcription polymerase chain reaction (qRT-PCR) analysis shows the relative expression level of genes involving in ovule primordia identity and initiation in *ckx3 ckx5* (**B**) and *bzr1-1D* (**C**) and under 30 min 1 μmol/L 6-BA and 30 min 1 μmol/L eBL treatment (**D**). Bars represent mean ± SD of three biological replicates (*n* = 15). Asterisks indicate significant difference (Student's two-tailed *t*-test: *P < 0.05; **P < 0.01).
Figure S2. Brassinosteroid (BR) enhances cytokinin (CK) signaling
Fluorescence signal of *TCS:GFP* (the reporter of cytokinin signaling) in roots of 4-DAG seedlings of Col, *bzr1-1D* and *bin2*$^{+/-}$ (scale bars, 50 μm).
Figure S3. BZR1 interacts with ARR1 but doesn't interact with ARR10
(**A**) Yeast two-hybrid assays show that BZR1 interacts with ARR10. (**B**) Bimolecular fluorescence complementation analyses reveal there are no interactions between ARR10 and BZR1 (scale bar, 50 μm). (**C**) Co-immunoprecipitation (Co-IP) assays show induction of ARR1 by brassinosteroid (BR) treatment and co-treatment with CK and BR. Co-IP assays illustrate interaction between BZR1 and ARR1, and induction of this interaction by 1 μmol/L BR treatment, 1 μmol/L CK and co-treatment with 1 μmol/L CK and 1 μmol/L BR. Western blots were conducted using tobacco co-expressing ARR1-mcherry and BZR1-GFP. Proteins were extracted from infiltrated leaves and detected using antibodies GFP and mCherry. (**D**) Immunoprecipitation assays showing induction of ARR1 transcription by cytokinin (CK) and co-treatment with CK and BR, and induction of BZR1 transcription by BR and co-treatment with CK and BR. Co-immunoprecipitation assays illustrating interaction between ARR1 and BZR1, and induction of this interaction by CK and co-treatment with CK and BR. Western blots were conducted using inflorescence of *pARR1::ARR1-GFP* seedlings. Proteins were extracted from infiltrated leaves and detected using antibodies to GFP and BZR1.
Figure S4. Enhanced cytokinin (CK) content partially rescues phenotypes of brassinosteroid (BR)-deficient mutant, but enhanced BR signal can't rescue CK-deficient mutant

(**A**) Seedlings (21 d after germination: DAG) of *det2* and three independent lines of *ckx3 ckx5 det2*. (**B**) Statistical analysis of silique length and seed number per silique (SNS) of *det2* and *ckx3 ckx5 det2*.

Bars represent mean $\pm$ SD of three biological replicates ($n = 30$). Asterisks indicate significant difference (Student's two-tailed t-test: $*P < 0.05$; $**P < 0.01$). (**C**) qRT-PCR analysis shows relative expression level of *CKX3* gene in Col, 35S:CKX3-GFP, *bzr1-1D*, *bzr1-1D* 35S:CKX3-GFP, DWF4-ox, and DWF4-ox 35S:CKX3-GFP. Bars represent mean $\pm$ SD of three biological replicates ($n = 30$). Asterisks indicate significant

difference (Student's two-tailed t-test: $*P < 0.05$; $**P < 0.01$). (**D**) Statistical analysis of seed number per silique of Col, *arr1* and *arr1 bzr1-1D*. Bars represent mean $\pm$ SD of three biological replicates ($n = 5$). Asterisks indicate significant difference (Student's two-tailed t-test: $*P < 0.05$; $**P < 0.01$).

Table S1. Primers used in this work

Scan using WeChat with your smartphone to view JIPB online

Scan with iPhone or iPad to view JIPB online